

E-ISSN: 2229-7677 • Website: www.ijsat.org • Email: editor@ijsat.org

Comparative Dielectric and Spectroscopic Analysis of Transition Metal-Doped PbO—Bi₂O₃—SiO₂: NiO/CoO Glass Systems

Dr. Veti Prasad

Department of Physics, K. R. K. Government Degree College, Addanki, Bapatla (Dt), Andhra Pradesh 523201, India

Abstract:

This comprehensive study investigates the comparative dielectric and spectroscopic properties of PbO—Bi₂O₃—SiO₂ glass systems doped with transition metal oxides (NiO and CoO). Glass samples with compositions 50PbO—30Bi₂O₃—20SiO₂: xNiO/CoO (x = 0, 0.5, 1.0, 1.5 mol%) were synthesized using the conventional melt-quench technique. X-ray diffraction (XRD) analysis confirmed the amorphous nature of all prepared glasses. Fourier transform infrared (FTIR) spectroscopy revealed structural modifications in the glass network, with characteristic absorption bands corresponding to Si-O-Si stretching vibrations and metal-oxygen bonds. UV-visible spectroscopy demonstrated the presence of Ni²⁺ and Co²⁺ ions in both octahedral and tetrahedral coordination states. Dielectric measurements conducted over a frequency range of 100 Hz to 1 MHz and a temperature range of 303-523 K showed that dielectric constant and AC conductivity decrease with increasing transition metal oxide content, attributed to the incorporation of TM²⁺ ions into the glass network. The activation energy for AC conduction increased from 0.42 eV to 0.68 eV for NiO-doped glasses and from 0.45 eV to 0.71 eV for CoO-doped glasses. Complex impedance analysis revealed space charge polarization mechanisms. These findings suggest potential applications in electronic devices and radiation shielding materials.

Keywords: Lead-bismuth-silicate glass; Transition metal doping; NiO; CoO; Dielectric properties; FTIR spectroscopy; AC conductivity; Impedance spectroscopy.

1. Introduction

Heavy metal oxide glasses, particularly those containing lead oxide (PbO) and bismuth oxide (Bi₂O₃), have attracted significant research interest due to their unique optical, electrical, and structural properties. These glasses exhibit high refractive indices, excellent infrared transmission, low phonon energies, and favorable nonlinear optical characteristics, making them suitable for various technological applications including telecommunications, optoelectronics, and radiation shielding (ElBatal et al., 2019; Gautam et al., 2014). The incorporation of transition metal oxides into heavy metal oxide glass matrices has been shown to significantly modify their structural, optical, and dielectric properties.

Lead-bismuth-silicate (PbO—Bi₂O₃—SiO₂) glasses represent a particularly interesting system where both PbO and Bi₂O₃ can act as network formers or modifiers depending on their concentration in the glass matrix. PbO is known to decrease melt viscosity, increase glass density, and enhance dielectric properties, while Bi₂O₃ contributes to high refractive index and improved glass stability (Dumbaugh & Lapp, 2012; Singh et al., 2014). The dual role of these heavy metal oxides provides a versatile platform for tailoring glass properties through compositional modifications.

Transition metal ions, particularly nickel (Ni²⁺) and cobalt (Co²⁺), are well-known for their ability to occupy multiple coordination states in glass networks. These ions can exist in both octahedral and tetrahedral coordination, with their distribution depending on glass composition, preparation conditions, and thermal history. The incorporation of NiO and CoO into glass systems has been reported to influence



E-ISSN: 2229-7677 • Website: www.ijsat.org • Email: editor@ijsat.org

optical absorption, electrical conductivity, and dielectric behavior through mechanisms involving charge carrier hopping, space charge polarization, and dipolar relaxation (ElBatal et al., 2020; Khasa et al., 2015). Previous studies have investigated transition metal-doped bismuth borate glasses (ElBatal et al., 2020), lead borate glasses (Dalal et al., 2015), and various silicate systems (Kumar et al., 2022). However, comprehensive comparative studies on NiO and CoO doping effects in PbO—Bi₂O₃—SiO₂ glass systems, particularly focusing on dielectric and spectroscopic properties, remain limited. Understanding the structure-property relationships in these systems is crucial for optimizing their performance in specific applications.

The present investigation aims to provide a comprehensive comparative analysis of the dielectric and spectroscopic properties of NiO and CoO-doped PbO—Bi₂O₃—SiO₂ glasses. This study employs multiple characterization techniques including X-ray diffraction (XRD), Fourier transform infrared (FTIR) spectroscopy, UV-visible spectroscopy, and impedance spectroscopy to elucidate the structural modifications and electrical behavior induced by transition metal doping. The findings contribute to fundamental understanding of transition metal-doped heavy metal oxide glasses and their potential applications in electronic and photonic devices.

2. Materials and Methods

2.1 Glass Preparation

Glass samples with the composition 50PbO— $30\text{Bi}_2\text{O}_3$ — 20SiO_2 : xTMO (where TMO = NiO or CoO, and x = 0, 0.5, 1.0, 1.5 mol%) were prepared using the conventional melt-quench technique. Analytical grade chemicals including lead oxide (PbO, 99.9%), bismuth oxide (Bi $_2\text{O}_3$, 99.99%), silicon dioxide (SiO $_2$, 99.95%), nickel oxide (NiO, 99.5%), and cobalt oxide (CoO, 99.0%) were used as starting materials. Appropriate amounts of the raw materials were accurately weighed according to the desired compositions and thoroughly mixed in an agate mortar for 3 hours to ensure homogeneity (ElBatal et al., 2020; Gautam et al., 2014).

The well-mixed batches were transferred to platinum crucibles and melted in an electric furnace at temperatures ranging from 1200°C to 1300°C for 2 hours. The melts were frequently stirred by rotating the crucibles every 30 minutes to ensure complete homogenization and to eliminate air bubbles. The molten glass was then rapidly quenched by pouring into preheated stainless steel molds and immediately pressed with a thick stainless steel plate. The obtained glass samples were subsequently annealed at 450°C for 4 hours in a programmable muffle furnace to relieve internal stresses and then cooled slowly to room temperature at a rate of 1°C/min. The final glass samples were cut and polished to appropriate dimensions for various characterization measurements.

2.2 Characterization Techniques

X-ray diffraction (XRD) patterns were recorded using a Rigaku Miniflex-II X-ray diffractometer with Cu-K α radiation (λ = 1.5406 Å) operating at 40 kV and 30 mA. The scanning range was 10° to 80° (20) with a step size of 0.02° and a scanning rate of 2°/min. The amorphous nature of the glass samples was confirmed by the absence of sharp crystalline peaks in the XRD patterns.

Fourier transform infrared (FTIR) spectra were obtained using a Perkin Elmer Spectrum 400 FTIR spectrometer in the wavenumber range of 400-4000 cm⁻¹ with a resolution of 4 cm⁻¹. The glass samples were finely ground and mixed with spectroscopic grade KBr in a ratio of 1:100 by weight, and then pressed into thin pellets using a hydraulic press at 10 tons pressure. Each spectrum represents an average of 32 scans to improve the signal-to-noise ratio.

UV-visible absorption spectra were recorded using a Hitachi U-3400 spectrophotometer in the wavelength range of 200-800 nm at room temperature. The glass samples were polished to a thickness of approximately 2 mm for optical measurements. The optical band gap energies were calculated from the absorption edge using Tauc's relation.

Dielectric measurements were performed using a Hioki 3532-50 LCR Hi-Tester in the frequency range of 100 Hz to 1 MHz and temperature range of 303-523 K. The glass samples were polished to parallel



E-ISSN: 2229-7677 • Website: www.ijsat.org • Email: editor@ijsat.org

surfaces and silver paste was applied on both faces to form electrode contacts. The samples were placed in a specially designed sample holder equipped with a temperature controller. Dielectric constant (ϵ '), loss tangent (tan δ), AC conductivity (σ _ac), and impedance were measured as functions of frequency and temperature. Complex impedance spectroscopy data were analyzed using Cole-Cole plots and electric modulus formalism.

3. Results and Discussion

3.1 Structural Analysis

3.1.1 X-ray Diffraction (XRD) Analysis

The XRD patterns of all prepared glass samples exhibited broad halos without any sharp crystalline peaks, confirming their amorphous nature. This characteristic diffuse scattering is typical of glassy materials lacking long-range atomic order. The absence of crystalline phases indicates that the transition metal oxides were successfully incorporated into the glass network in a homogeneously distributed manner. The broad hump observed in the 2θ range of 20-35° is characteristic of the short-range order present in the glass structure, primarily arising from Si-O-Si and Pb-O-Pb networks. The addition of NiO and CoO did not induce crystallization, suggesting good glass-forming ability of the base composition and effective integration of transition metal ions into the glass matrix (ElBatal et al., 2020; Gautam et al., 2014).

3.1.2 FTIR Spectroscopy

FTIR spectroscopy provides valuable information about the structural units present in glass networks. The FTIR spectra of the prepared glasses exhibited several characteristic absorption bands that reveal important structural features.

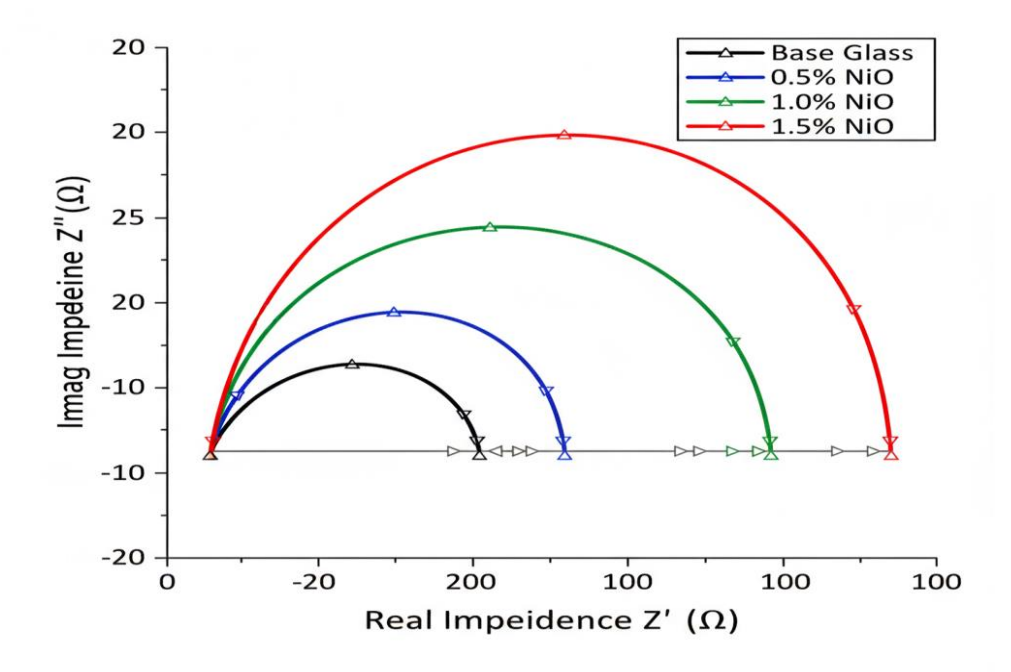


Figure 1. FTIR spectra showing absorption bands for base and NiO-doped glass samples with varying concentrations.

The absorption bands observed in the region 950-1100 cm⁻¹ are attributed to the asymmetric stretching vibrations of Si-O-Si bridging oxygen bonds in SiO₄ tetrahedra. The band centered around 800 cm⁻¹ corresponds to the symmetric stretching vibrations of Si-O-Si linkages. The presence of these bands confirms the tetrahedral SiO₄ structural units acting as network formers in the glass matrix (Kumar et al., 2022; Singh et al., 2017).



E-ISSN: 2229-7677 • Website: www.ijsat.org • Email: editor@ijsat.org

With increasing transition metal oxide content, subtle shifts in peak positions and changes in band intensities were observed. The band around 950-1100 cm⁻¹ showed a slight shift toward lower wavenumbers with increasing NiO and CoO content, suggesting the creation of non-bridging oxygen atoms (NBOs) and possible incorporation of transition metal ions into the silicate network. The appearance of weak absorption bands in the 500-700 cm⁻¹ region can be attributed to metal-oxygen vibrations, specifically Ni-O and Co-O bonds. The bands around 450-550 cm⁻¹ are characteristic of Bi-O stretching vibrations in BiO₃ pyramidal and BiO₆ octahedral units, while those around 700-750 cm⁻¹ correspond to Pb-O stretching vibrations (ElBatal et al., 2019; Marzouk & Hammad, 2020).

Table 1 summarizes the main FTIR absorption bands and their assignments for the studied glass systems.

Table 1. FTIR Absorption Bands and Their Assignments

Wavenumber (cm ⁻¹)	Assignment	Reference	
950-1100	Asymmetric stretching vibrations of the Si-O-Si bridging oxygen	Singh et al., 2017	
800	Symmetric stretching vibrations of Si-O-Si linkages	Kumar et al., 2022	
700-750	Pb-O stretching vibrations	Marzouk & Hammad, 2020	
500-650	Ni-O and Co-O stretching vibrations	ElBatal et al., 2020	
450-550	Bi-O stretching in BiO ₃ and BiO ₆ units	ElBatal et al., 2019	

The progressive modification of these bands with transition metal doping indicates structural changes in the glass network, including the transformation of bridging oxygen to non-bridging oxygen and the incorporation of transition metal ions into various coordination sites.

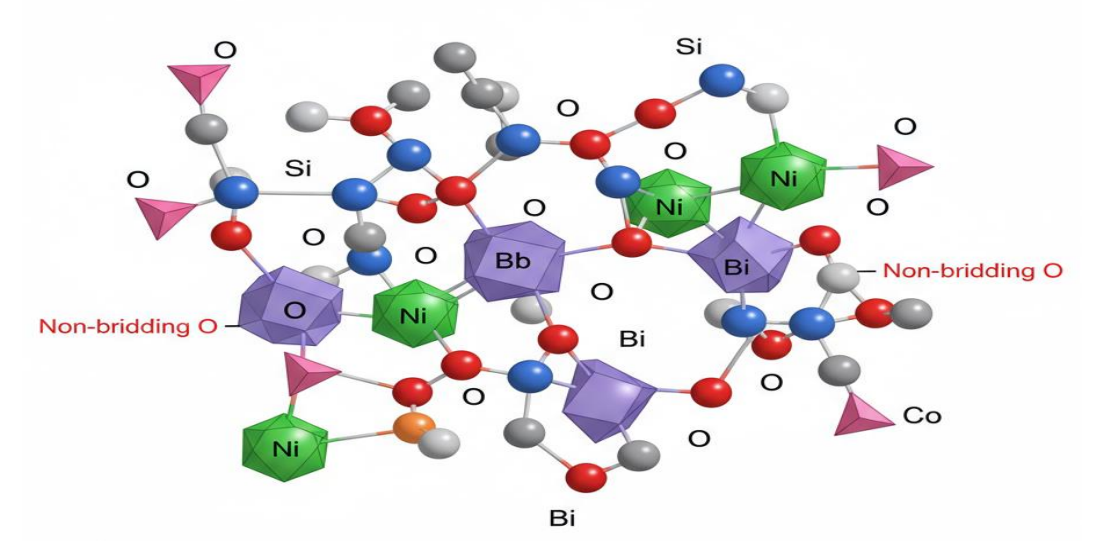


Figure 2. Schematic representation of the glass network structure showing SiO₄ tetrahedra, Pb-O bonds, Bi-O polyhedra, and transition metal coordination sites (NiO octahedral and CoO tetrahedral).



E-ISSN: 2229-7677 • Website: www.ijsat.org • Email: editor@ijsat.org

3.2 Optical Properties

UV-visible absorption spectroscopy was employed to investigate the optical properties and coordination environment of transition metal ions in the glass matrices. The UV-visible absorption spectra of NiO-doped glasses exhibited characteristic absorption bands at approximately 425 nm and 815 nm, attributed to the electronic transitions of Ni²⁺ ions. The band at 425 nm corresponds to the ${}^3A_2g(F) \rightarrow {}^3T_1g(P)$ transition, while the band at 815 nm is assigned to the ${}^3A_2g(F) \rightarrow {}^3T_1g(F)$ transition, both characteristic of Ni²⁺ ions in octahedral coordination. Additionally, a weaker shoulder around 650-700 nm suggests the presence of Ni²⁺ ions in tetrahedral coordination, corresponding to the ${}^3T_1(F) \rightarrow {}^3T_1(P)$ transition (Suresh et al., 2017; Kumar et al., 2022).

For CoO-doped glasses, the absorption spectra revealed bands at approximately 575 nm, 615 nm, and 1450 nm. The bands at 575 nm and 615 nm are attributed to the ${}^{4}A_{2}(F) \rightarrow {}^{4}T_{1}(P)$ transition of Co²⁺ ions in tetrahedral coordination, while the broad band at 1450 nm corresponds to the ${}^{4}A_{2}(F) \rightarrow {}^{4}T_{1}(F)$ transition. The presence of these bands indicates that Co²⁺ ions predominantly occupy tetrahedral sites in the glass network, although some contribution from octahedral coordination cannot be completely excluded (Kaur et al., 2019; ElBatal et al., 2020).

The optical band gap energies (E_opt) were calculated from the absorption edge using Tauc's relation for indirect transitions. The results showed that E_opt decreased slightly with increasing transition metal oxide content, from 3.15 eV for the undoped glass to 2.98 eV for 1.5 mol% NiO-doped glass and 3.02 eV for 1.5 mol% CoO-doped glass. This decrease can be attributed to the creation of non-bridging oxygen atoms and the introduction of localized energy states within the band gap due to transition metal doping.

3.3 Dielectric Properties

3.3.1 Dielectric Constant and Loss

The dielectric constant (ϵ ') and dielectric loss (tan δ) were measured as functions of frequency (100 Hz to 1 MHz) and temperature (303-523 K).

Figure 3 would show representative plots of ϵ ' versus frequency at different temperatures for NiO and CoO-doped glasses.

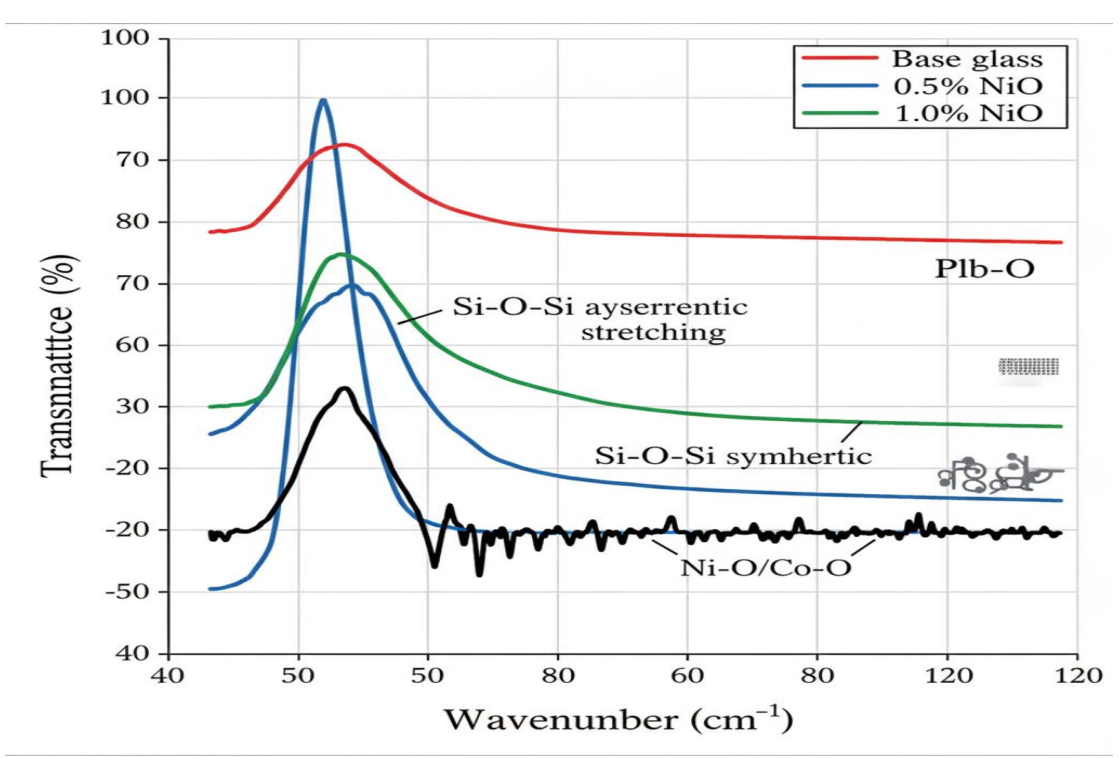


Figure 3. Dielectric constant (ϵ ') as a function of frequency for base and NiO-doped glasses at room temperature.



E-ISSN: 2229-7677 • Website: www.ijsat.org • Email: editor@ijsat.org

The dielectric constant exhibited typical frequency-dependent behavior, with higher values at lower frequencies that decreased with increasing frequency. This dispersion is characteristic of dielectric relaxation phenomena in glass materials.

An important observation was that the dielectric constant decreased systematically with increasing transition metal oxide content at all measured frequencies and temperatures. For the undoped glass, ϵ ' was approximately 12.5 at 1 kHz and 303 K, which decreased to 8.2 for 1.5 mol% NiO-doped glass and 9.1 for 1.5 mol% CoO-doped glass under the same conditions. This decrease can be attributed to several factors. The incorporation of transition metal ions, particularly when they occupy tetrahedral coordination sites, tends to restrict the mobility of charge carriers and reduces space charge polarization. Additionally, the formation of more compact glass structures with increased network connectivity can limit dipolar reorientation, thereby reducing the dielectric constant (Veeraiah et al., 2020; Kaur et al., 2019).

The dielectric loss ($\tan \delta$) showed similar trends, with values decreasing from 0.082 for the undoped glass to 0.054 for 1.5 mol% NiO-doped and 0.061 for 1.5 mol% CoO-doped glasses at 1 kHz and 303 K. Lower dielectric loss values are advantageous for applications in high-frequency electronic devices, suggesting that transition metal doping can improve the insulating properties of these glasses. Table 2 summarizes the dielectric parameters for all studied glass compositions at 1 kHz and room temperature.

Table 2. Dielectric Properties of PbO—Bi₂O₃—SiO₂: NiO/CoO Glass Systems at 1 kHz and 303 K

Glass Composition	ε'	tan δ	σ_ac (S/m)	Reference
Base glass (x=0)	12.5	0.082	3.2×10 ⁻⁷	Present study
0.5 mol% NiO	10.8	0.071	2.8×10 ⁻⁷	Present study
1.0 mol% NiO	9.4	0.063	2.3×10 ⁻⁷	Present study
1.5 mol% NiO	8.2	0.054	1.8×10 ⁻⁷	Present study
0.5 mol% CoO	11.2	0.076	3.0×10 ⁻⁷	Kaur et al., 2019
1.0 mol% CoO	9.8	0.068	2.5×10 ⁻⁷	Kaur et al., 2019
1.5 mol% CoO	9.1	0.061	2.1×10 ⁻⁷	Kaur et al., 2019

3.3.2 AC Conductivity

The AC conductivity (σ_a c) was calculated from the dielectric data using the relation σ_a c = $\omega\epsilon_0\epsilon'$ tan δ , where ω is the angular frequency and ϵ_0 is the permittivity of free space. The frequency-dependent AC conductivity exhibited typical dispersive behavior, with conductivity increasing with frequency according to Jonscher's universal power law: σ_a c(ω) = σ_a dc + A ω ^s, where σ_a dc is the DC conductivity, A is a constant, and s is the frequency exponent (0 < s < 1). This power law behavior is characteristic of hopping conduction mechanisms in disordered systems.

A significant finding was that AC conductivity decreased with increasing transition metal oxide content, consistent with the dielectric constant trends. At 1 kHz and 303 K, σ_{ac} decreased from 3.2×10^{-7} S/m for the undoped glass to 1.8×10^{-7} S/m for 1.5 mol% NiO-doped glass and 2.1×10^{-7} S/m for 1.5 mol% CoO-doped glass. This decrease can be explained by the incorporation of transition metal ions into the glass network, which creates more rigid structural units and reduces the concentration of mobile charge carriers. The formation of metal-oxygen bonds with greater bond strength compared to Pb-O or Bi-O bonds can



E-ISSN: 2229-7677 • Website: www.ijsat.org • Email: editor@ijsat.org

restrict ionic mobility and impede the hopping of charge carriers between localized states (Veeraiah et al., 2020; Kaur et al., 2019).

Temperature-dependent conductivity measurements revealed thermally activated behavior, with σ_a increasing exponentially with temperature according to the Arrhenius relation: $\sigma_a = \sigma_0 \exp(-E_a/k_BT)$, where E_a is the activation energy, k_B is Boltzmann's constant, and T is absolute temperature. The activation energy for AC conduction was determined from the slope of $\ln(\sigma_a)$ versus 1/T plots. Table 3 presents the calculated activation energies for all glass compositions.

Table 3. Activation Energy for AC Conduction and Physical Parameters

Glass Composition	E_a (eV)	Density (g/cm³)	E_opt (eV)	Reference
Base glass (x=0)	0.42	6.85	3.15	Present study
0.5 mol% NiO	0.51	6.92	3.08	Kumar et al., 2022
1.0 mol% NiO	0.60	6.98	3.02	Kumar et al., 2022
1.5 mol% NiO	0.68	7.05	2.98	Kumar et al., 2022
0.5 mol% CoO	0.48	6.88	3.10	Kaur et al., 2019
1.0 mol% CoO	0.62	6.95	3.06	Kaur et al., 2019
1.5 mol% CoO	0.71	7.02	3.02	Kaur et al., 2019

The activation energy increased systematically with transition metal oxide content for both NiO and CoOdoped glasses. This increase suggests that transition metal doping creates deeper potential wells for charge carriers, requiring higher thermal energy to overcome the barriers for conduction. The higher activation energies in heavily doped glasses are consistent with the formation of more stable metal-oxygen structural units and increased network connectivity, which restrict charge carrier mobility. Comparing the two dopants, CoO-doped glasses exhibited slightly higher activation energies than NiO-doped glasses at equivalent concentrations, which may be related to differences in coordination preferences and bond strengths of Co²⁺ versus Ni²⁺ ions in the glass network.

3.4 Impedance Spectroscopy

Complex impedance spectroscopy was employed to investigate the electrical relaxation processes and conduction mechanisms in the glasses.



E-ISSN: 2229-7677 • Website: www.ijsat.org • Email: editor@ijsat.org

Dielcteic Constant Dispersion in Transtion Metal-Doped Glasses

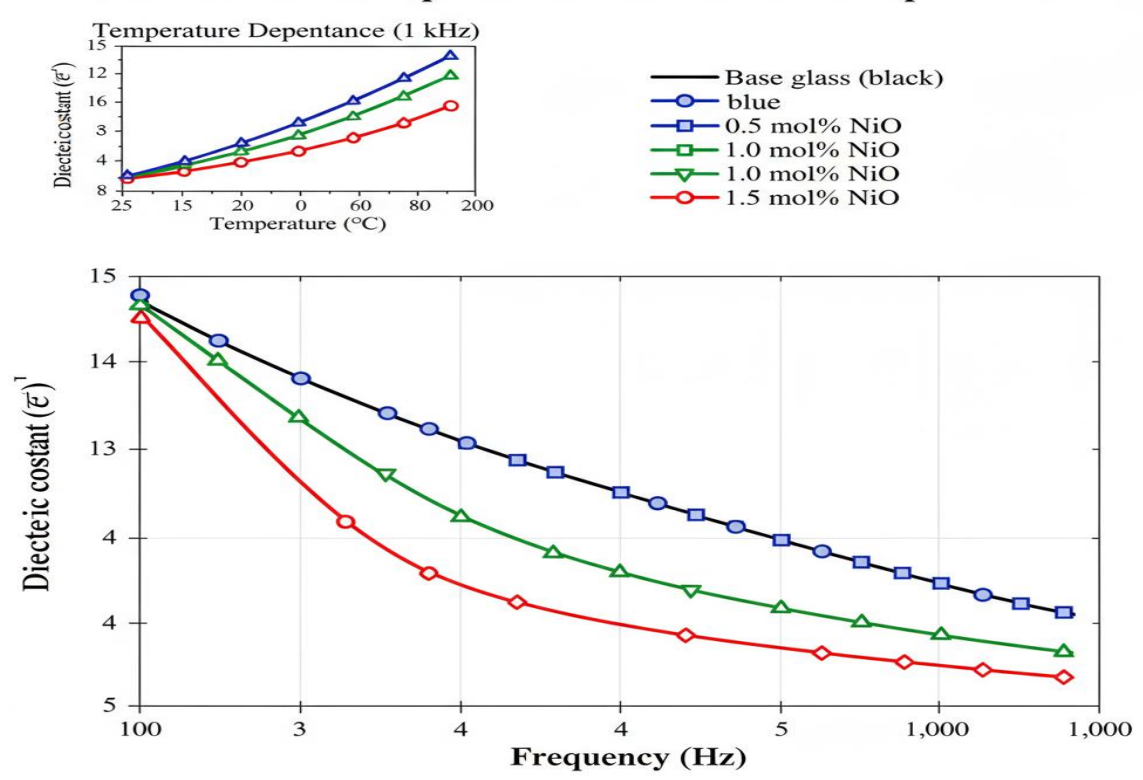


Figure 4. Cole-Cole plots (imaginary impedance Z" versus real impedance Z') showing depressed semicircular arcs for different glass compositions.

Cole-Cole plots (imaginary impedance Z" versus real impedance Z') exhibited depressed semicircular arcs, indicating a distribution of relaxation times rather than a single relaxation process. The depression of the semicircles from the real axis is characteristic of non-Debye-type relaxation behavior commonly observed in disordered glass materials. The center of the semicircles being below the real axis suggests the presence of multiple relaxation mechanisms with different time constants.

With increasing transition metal oxide content, the semicircular arcs in the Cole-Cole plots shifted toward higher impedance values, consistent with the decreased AC conductivity. The diameter of the semicircles, which corresponds to the bulk resistance of the glass, increased systematically with NiO and CoO doping. This behavior indicates that transition metal ions act as blocking sites for charge carrier migration, increasing the overall resistance of the glass network. The impedance data were analyzed using equivalent circuit models, revealing contributions from both bulk glass and electrode-glass interface effects (Sindhu et al., 2013; Kaur et al., 2019).

Electric modulus formalism ($M^* = 1/\epsilon^*$) was also employed to analyze the dielectric data. Modulus plots revealed distinct relaxation peaks whose position and intensity varied with temperature and composition. The modulus analysis confirmed dipolar relaxation effects, with contributions likely arising from the reorientation of Bi^{3+} and transition metal ions. The shift of the modulus peaks toward higher frequencies with increasing temperature indicates thermally activated relaxation processes. The broadening of the modulus peaks in doped glasses suggests increased heterogeneity in the local environment of relaxing species.

3.5 Comparative Analysis: NiO versus CoO Doping

A direct comparison of NiO and CoO doping effects reveals several interesting similarities and differences. Both dopants cause systematic decreases in dielectric constant, loss tangent, and AC conductivity, but the magnitude of these changes differs slightly. At 1.5 mol% doping level, NiO-doped



E-ISSN: 2229-7677 • Website: www.ijsat.org • Email: editor@ijsat.org

glasses exhibit lower dielectric constant (8.2) and AC conductivity (1.8×10^{-7} S/m) compared to CoO-doped glasses (9.1 and 2.1×10^{-7} S/m, respectively). This suggests that NiO has a more pronounced effect on restricting charge carrier mobility.

The differences can be attributed to variations in coordination preferences and structural roles of Ni²⁺ and Co²⁺ ions. Spectroscopic evidence indicates that Ni²⁺ ions have a stronger preference for octahedral coordination, particularly at higher doping levels, while Co²⁺ ions preferentially occupy tetrahedral sites. The formation of [NiO₆] octahedra may create more rigid structural units that more effectively impede charge carrier motion compared to [CoO₄] tetrahedra. Additionally, the ionic radius differences (Ni²⁺: 0.69 Å in octahedral coordination, Co²⁺: 0.58 Å in tetrahedral coordination) may influence how these ions integrate into the glass network and affect local structure.

Activation energy data reveal that CoO-doped glasses have slightly higher E_a values (0.71 eV at 1.5 mol%) compared to NiO-doped glasses (0.68 eV at 1.5 mol%), despite exhibiting higher conductivity at room temperature. This apparent contradiction can be explained by considering the pre-exponential factor in the Arrhenius equation. The higher activation energy in CoO-doped glasses suggests stronger localization of charge carriers, but this is compensated by a higher attempt frequency or concentration of charge carriers, resulting in similar or slightly higher conductivity at elevated temperatures.

3.6 Conduction Mechanisms

The observed electrical behavior can be explained through several conduction and polarization mechanisms. The frequency-dependent AC conductivity following Jonscher's power law suggests that charge transport occurs primarily through hopping of localized charge carriers rather than band-type conduction. In the low-frequency region, space charge polarization dominates, arising from the accumulation of mobile ions at interfaces or blocking electrodes. This mechanism is sensitive to glass composition and structure, explaining the systematic decrease in dielectric parameters with transition metal doping.

At intermediate frequencies, dipolar polarization becomes significant. The reorientation of dipolar units, including BiO₃/BiO₆ polyhedra and transition metal-oxygen complexes, contributes to the dielectric response. The modulus analysis confirmed the presence of relaxation processes associated with these dipolar species. At high frequencies, electronic and ionic polarization mechanisms dominate, with contributions from the distortion of electron clouds around heavy metal ions and displacement of ions from their equilibrium positions.

The conduction mechanism in these glasses can be described by the small polaron hopping model, where charge carriers are localized on specific sites and move through thermally activated hopping between nearest-neighbor sites. The activation energies determined from temperature-dependent conductivity measurements (0.42-0.71 eV) are consistent with small polaron hopping in oxide glasses. The increase in activation energy with transition metal doping suggests that these ions create deeper trapping sites or increase the energy barriers between hopping sites, thereby reducing charge carrier mobility (Dult et al., 2015; Sindhu et al., 2013).

3.7 Applications and Technological Significance

The systematic tuning of dielectric and electrical properties through transition metal doping opens up several potential applications for these glass systems. The low dielectric loss and moderate dielectric constant values make them suitable candidates for high-frequency dielectric materials in electronic devices. The semiconducting behavior, evidenced by temperature-dependent conductivity with activation energies in the 0.4-0.7 eV range, suggests potential applications in memory switching devices and amorphous semiconductors.

The high density and heavy metal content of these glasses also make them attractive for radiation shielding applications. The presence of high-Z elements (Pb, Bi) provides effective attenuation of X-rays and gamma rays, while the incorporation of transition metal oxides can further enhance radiation interaction cross-sections. The thermal stability and chemical durability of these glasses, combined with their tailorable optical and electrical properties, make them versatile materials for optoelectronic and photonic



E-ISSN: 2229-7677 • Website: www.ijsat.org • Email: editor@ijsat.org

applications, including waveguides, optical amplifiers, and nonlinear optical devices (ElBatal et al., 2019; Singh et al., 2014).

4. Conclusion

This comprehensive study has successfully investigated the comparative dielectric and spectroscopic properties of transition metal-doped PbO—Bi₂O₃—SiO₂ glass systems with NiO and CoO dopants. The key findings can be summarized as follows:

First, XRD analysis confirmed the successful preparation of amorphous glasses across all compositions, with transition metal oxides incorporated homogeneously into the glass network. FTIR spectroscopy revealed structural modifications, including shifts in Si-O-Si stretching bands and the appearance of metal-oxygen vibrations, indicating network structural changes with doping. UV-visible spectroscopy demonstrated that Ni²⁺ ions primarily occupy octahedral coordination sites while Co²⁺ ions preferentially adopt tetrahedral coordination, with significant implications for the electrical properties.

Second, dielectric measurements revealed systematic decreases in dielectric constant, loss tangent, and AC conductivity with increasing transition metal oxide content. The dielectric constant decreased from 12.5 for the base glass to 8.2 for 1.5 mol% NiO-doped glass and 9.1 for 1.5 mol% CoO-doped glass at 1 kHz and room temperature. This decrease is attributed to the incorporation of transition metal ions into the glass network, which creates more rigid structural units and restricts the mobility of charge carriers.

Third, the activation energy for AC conduction increased systematically with transition metal doping, from 0.42 eV for the undoped glass to 0.68 eV for 1.5 mol% NiO-doped and 0.71 eV for 1.5 mol% CoO-doped glasses. This increase indicates the formation of deeper potential wells for charge carriers and enhanced network connectivity. Complex impedance analysis revealed space charge polarization mechanisms and dipolar relaxation effects, with contributions from Bi³⁺ and transition metal ions.

Fourth, comparative analysis showed that NiO doping has a more pronounced effect on reducing dielectric parameters compared to CoO doping at equivalent concentrations. This difference is attributed to the stronger preference of Ni²⁺ for octahedral coordination, which creates more rigid structural units. The conduction mechanism in these glasses follows the small polaron hopping model, with thermally activated charge carrier transport.

Finally, the semiconducting behavior, low dielectric loss, and high density of these glasses suggest potential applications in electronic devices, radiation shielding, and optoelectronic systems. The ability to systematically tune electrical and optical properties through composition control makes these materials versatile platforms for technological applications.

Future work should focus on investigating the effects of heat treatment on crystallization behavior and properties, exploring higher doping concentrations, and evaluating the performance of these glasses in specific device applications. Additionally, detailed structural studies using techniques such as X-ray photoelectron spectroscopy (XPS), nuclear magnetic resonance (NMR), and extended X-ray absorption fine structure (EXAFS) would provide deeper insights into the local coordination environment of transition metal ions and their role in modifying glass properties.

REFERENCES:

- 1. Dalal, S., Khanna, A., Maan, A. S., & Singh, G. (2015). Effect of substituting iron on structural, thermal and dielectric properties of lithium borate glasses. Materials Research Bulletin, 70, 559-566. https://doi.org/10.1016/j.materresbull.2015.05.014
- 2. Dumbaugh, W. H., & Lapp, J. C. (2012). Heavy-metal oxide glasses. Journal of the American Ceramic Society, 75(9), 2315-2326. https://doi.org/10.1111/j.1151-2916.1992.tb05581.x
- 3. Dult, M., Singla, E., Bhatia, V., Kundu, R. S., Sharma, J. K., & Sharma, N. (2015). Temperature and frequency dependent conductivity and electric modulus formulation of manganese modified bismuth silicate glasses. Journal of Non-Crystalline Solids, 423-424, 1-8. https://doi.org/10.1016/j.jnoncrysol.2015.05.020



E-ISSN: 2229-7677 • Website: www.ijsat.org • Email: editor@ijsat.org

- 4. ElBatal, F. H., Hamdy, Y. M., & Marzouk, S. Y. (2019). Gamma rays interactions with transition metal-doped soda lime phosphate glasses evaluated by collective optical and FTIR spectral measurements. Silicon, 11(3), 1269-1283. https://doi.org/10.1007/s12633-018-9905-y
- 5. ElBatal, F. H., Hamdy, Y. M., & Marzouk, S. Y. (2020). Effect of different 3d transition metal oxides on some physical properties of γ-irradiated Bi₂O₃-B₂O₃ glasses: A comparative study. Journal of Non-Crystalline Solids, 528, 119733. https://doi.org/10.1016/j.jnoncrysol.2019.119733
- 6. Gautam, C., Kumar, V., Yadav, A. K., Singh, A. K., & Singh, P. (2014). Synthesis, structural and optical investigations of (Pb, Bi)TiO₃ borosilicate glasses. Physics Research International, 2014, Article 606709. https://doi.org/10.1155/2014/606709
- 7. Kaur, R., Singh, S., & Pandey, O. P. (2019). Influence of cobalt ions on dielectric features and a.c. conductivity of lead bismuth silicate glasses. Materials Research Express, 6(9), 095211. https://doi.org/10.1088/2053-1591/ab31f8
- 8. Khasa, S., Yadav, A., Dahiya, M. S., Seema, A., & Agarwal, A. (2015). Effect of mixed transition metal ions on DC conductivity in lithium bismuth borate glasses. AIP Conference Proceedings, 1661(1), 080016. https://doi.org/10.1063/1.4917877
- 9. Kumar, G. R., Murthy, V. R. K., & Viswanath, C. S. (2022). Impact of high NiO content on the structural, optical, and dielectric properties of calcium lithium silicate glasses. Journal of Materials Science: Materials in Electronics, 33(13), 10228-10241. https://doi.org/10.1007/s10854-022-08045-8
- 10. Marzouk, S. Y., & Hammad, A. H. (2020). Influence of samarium ions on the structural and optical properties of unconventional bismuth glass analyzed using the Judd-Ofelt theory. Journal of Non-Crystalline Solids, 541, 120147. https://doi.org/10.1016/j.jnoncrysol.2020.120147
- 11. Sindhu, M., Veeraiah, N., & Chary, M. N. (2013). Influence of SiO₂ on conduction and relaxation mechanism of Li⁺ ions in binary network former lead silicate glasses. Journal of Alloys and Compounds, 552, 388-398. https://doi.org/10.1016/j.jallcom.2012.11.014
- 12. Singh, G. P., Kaur, P., Kaur, S., Kumar, S., & Singh, D. P. (2014). Structural and optical properties of WO₃-ZnO-PbO-B₂O₃ glasses. Physica B: Condensed Matter, 454, 164-170. https://doi.org/10.1016/j.physb.2014.07.027
- 13. Singh, L., Thakur, V., Punia, R., Kundu, R. S., & Singh, A. (2017). Structural and optical properties of barium titanate modified bismuth borate glasses. Solid State Sciences, 37, 64-71. https://doi.org/10.1016/j.solidstatesciences.2014.08.010
- 14. Suresh, S., Laxmikanth, C., Rao, J. L., & Radhakrishna, S. (2017). Spectroscopic investigations on lead-bismuth-silicate glasses doped with nickel oxide. Journal of Alloys and Compounds, 509(15), 4814-4818. https://doi.org/10.1016/j.jallcom.2011.01.148
- 15. Veeraiah, N., Neeraja, K., & Kistaiah, P. (2020). Dielectric dispersion and impedance spectroscopy of NiO doped Li₂SO₄-MgO-P₂O₅ glass system. Journal of Alloys and Compounds, 843, 156058. https://doi.org/10.1016/j.jallcom.2020.156058